frontiers | Frontiers in Coatings, Dyes and Interface Engineering

TYPE Original Research
PUBLISHED 31 January 2025
DOI 10.3389/frcdi.2025.1527060

OPEN ACCESS

EDITED BY
Jose L. Endrino,
Loyola Andalusia University, Spain

REVIEWED BY
Nesimi Uludag,
Namik Kemal University, Türkiye
Ely Dannier Valbuena Niño,
Fundación of Researchers in Science and Technology of Materials, Colombia

*CORRESPONDENCE
María Fernanda Cerdá,
fcerda@fcien.edu.uy

RECEIVED 12 November 2024
ACCEPTED 09 January 2025
PUBLISHED 31 January 2025

CITATION
Ávila M and Cerdá MF (2025) Thermodynamic and kinetics considerations in the competition between the dye regeneration and the recombination process in dye-sensitized solar cells.
Front. Coat. Dyes Interface Eng. 3:1527060.
doi: 10.3389/frcdi.2025.1527060

Thermodynamic and kinetics considerations in the competition between the dye regeneration and the recombination process in dye-sensitized solar cells

Mauricio Ávila and María Fernanda Cerdá*

Laboratorio de Biomateriales, Instituto de Química Biológica, Facultad de Ciencias UdelaR, Montevideo, Uruguay

Dye-sensitized solar cells comprise a fluorine doped tin oxide/titanium dioxide photoanode and a counter electrode of fluorine doped tin oxide covered with a catalytic material arranged in a sandwich configuration. Many processes take place inside a dye-sensitized solar cell. However, two involve the redox couple contained in the electrolyte solution: the dye regeneration and the recombination. While the first is a desired path, the latter impacts the power conversion efficiency of the cells, decreasing the measured values. In this work, iodine-based couples are evaluated using cyclic voltammetric measurements, and their behaviour is compared with two commercial electrolytes widely used in dye-sensitized solar cells, particularly when sensitized with natural dyes. Different experimental conditions, such as cell configurations and electrode materials, were adopted to understand the thermodynamics of the competitive electron transfer processes mentioned above.

KEYWORDS

iodine, electrochemistry, redox potential, pigments, redox balance

1 Introduction

Dye-sensitized solar cells (DSSC) were reported for the first time in the 90's, followed by explosive attention from several research groups and generating thousands of reports (O'Regan and Grätzel, 1991; Bisquert et al., 2004; Boschloo, 2019; Zhang et al., 2021; Zou et al., 2022; Khan et al., 2023; Ren et al., 2023; Montagni et al., 2024; Spadaro et al., 2024). After reaching power conversion efficiencies comparable to or higher than those obtained from silicon-traditional ones (Hamed et al., 2017; Sharma et al., 2018; Ferdowsi et al., 2020; Francis and Ikenna, 2021; Baby et al., 2022; Ren et al., 2023; Korir et al., 2024), the attention about the topic focused around the particular characteristics of DSSC and their related fields of applications (Dai et al., 2008; Aslam et al., 2020; Devadiga et al., 2021; Hyun et al., 2022; Barichello et al., 2024; Chandra Sil et al., 2020). Many companies around the world offer their products in the Market, with some of them responsible for the inclusion of DSSC in buildings such as the Swiss Convention Center of Lausanne, the Science Tower in Austria or the Solar Pavilion at Roskilde University in Denmark (Barichello et al., 2024).

DSSC are sandwich cells with two flat electrodes of conductive glass as FTO (Fluorine-doped Tin Oxide). One is the photoanode, composed of nanostructured mesoporous titanium dioxide (TiO_2) deposited onto the FTO and dyes adsorbed onto its surface, whereas the counter consists

typically of an FTO/platinum (Pt) electrode (Uludag et al., 2018). Between them, an electrolyte containing a redox couple is placed. The working principle involves electron generation and transfer after the sunlight reaches the dye. When the light reaches the dye, electrons are promoted from the HOMO (Highest Occupied Molecular Orbital) to the LUMO (Lowest Unoccupied Molecular Orbital) orbital of the pigment. Then, electron transference to the TiO_2 occurs according to the thermodynamic balance between the semiconductor's LUMO potential and the Fermi potential. Then, electrons are transferred to the FTO surface, and they move to the counter FTO/Pt electrode, where they are caught by the redox iodine-related couple. The cycle finishes when the oxidized form of the dye is regenerated by the redox couple of the electrolyte (Jasim, 2011; Jiao et al., 2011; Sharma et al., 2018; Muñoz-García et al., 2021).

The dyes must completely fit several characteristics to be applied as sensitizers (Alhmed et al., 2012; Basheer et al., 2014; Shalini et al., 2016; Arifin et al., 2017; Semalti and Sharma, 2020; Sen et al., 2023). Among them, the dye has to reach an adequate redox potential to ensure the regeneration of the oxidized form of the dye by a couple of the electrolytes (Daeneke et al., 2012; Jeon et al., 2014; Masud, 2023). Several redox couples have been reported to be used in the electrolytes of the DSSC (Boschloo and Hagfeldt, 2009; Ates et al., 2012; Sun et al., 2015; Zhou et al., 2020). The iodide/triiodide (I^-/I_3^-) redox is widely used, giving still the most stable and efficient DSCC (Popov and Deskin, 1958; Dané et al., 1968; Baucke et al., 1971; Stanbury et al., 1980; Stanbury, 1989; Wang and Stanbury, 2006; Boschloo and Hagfeldt, 2009; Yanagida et al., 2009; Robson et al., 2012; Dhonde et al., 2022). This couple shows many favourable characteristics, i.e., good solubility and suitable redox potential, providing rapid dye regeneration. The couple also has very slow recombination kinetics with the electrons in TiO_2 (Boschloo et al., 2011). But which electron exchanges are involved inside a DSSC? The iodine/iodide system is very complex, and several couples can be considered. Generally, the oxidizing redox potential associated with the dye is around 1 V, and different iodine-related species can be regarded to ensure an adequate energy balance inside the DSSC. The iodide system has been widely evaluated, several couples have been reported, and many reports are based on the use of electrocatalytic materials such as platinum or gold (Rodriguez and Soriaga, 1988).

This work reports the complete voltammetric evaluation of the different iodine-related species involved in different redox potentials. Different electrolytes and electrode materials are applied. Also, two of the most utilized electrolytes when using natural sensitizers are characterized. Which couples are involved in dye's regeneration? Are all iodine-related species suitable to ensure this regeneration? To answer these questions, thermodynamics and kinetics considerations will be addressed here.

2 Materials and methods

All reagents were used as received from commercial sources. Experiments were carried out using a Metrohm μStat-i 400 s Potentiostat. The voltammetric profiles of the systems were evaluated in two different supporting electrolytes: acetonitrile solution with 0.04 M tetramethylammonium perchlorate ($C_4H_{12}NClO_4$) and in aqueous 0.1 M sodium perchlorate ($NaClO_4$), in MilliQ 18.2 MΩ water. Voltammetric measurements were carried out in 1- a one-compartment conic cell, using a polycrystalline gold disc (Au-*pc*, 3 mm diameter) as working electrode, FTO or FTO/TiO_2 electrodes (0.77 cm^2 geometric area), a Pt sheet as counter electrode and a calomel saturated electrode (SCE) as the reference; and 2- using screen-printed gold electrodes (Dropsens/Metrohm, 220BT and ITO10). When using screen-printed electrodes, also two different methodologies were applied: the traditional drop-mode (SPD) (Morrin et al., 2003; García-Miranda et al., 2021; Wang et al., 2022; Kelíšková et al., 2023) and the thin-layer mode (SPTL) (Hubbard, 1969; Botasini et al., 2016; Tanner and Compton, 2018; Marzouk et al., 2021). For the last one, a cover glass is deposited onto the screen-printed electrode where the drop is deposited, and the "sandwich" is pressed with office clips.

Different electrochemical routines were applied: (a) cyclic voltammetry run at scan rates ν varying between 0.01 V s^{-1} and 0.05 V s^{-1} from a cathodic switching potential Ec to an anodic switching potential Ea, and (b) repetitive triangular potential scans at $\nu = 0.05$ V s^{-1} with either constant Ec and gradual changes of Ea or constant Ea and gradual changes of Ec. The ferrocene/ferrocenium (Fc/Fc^+) redox couple in acetonitrile solutions and the ferrocyanide/ferricyanide ($[Fe(CN)_6]^{3-}/([Fe(CN)_6]^{4-}$) redox couple in aqueous solutions were utilized to assess the value of the reference electrode when using the screen-printed ones. To evaluate the redox couples, 1 mM potassium iodide (KI) solutions in the supporting electrolytes were analyzed.

Finally, two electrolytes applied in DSSC were evaluated: iodolyte AN50$^{(R)}$ (Solaronix, 50 mM 1,2-dimethyl-3-propylimidazolium iodide in acetonitrile) and one named "ACVAL" (Lithium iodide, LiI, 0.8 M + iodine, I_2, 0.05 M in a mixture 85/15 acetonitrile/valeronitrile). These two commercial electrolyte solutions were diluted with acetonitrile to get a final concentration of 1 mM in iodide and to compare the results with those obtained from the 1 mM KI solutions.

All potentials in the text are referred to the normal hydrogen electrode (NHE).

3 Results and discussion

As explained above, measured potentials were corrected using a redox couple as a reference. The potential values presented in this section are all reported against the NHE.

Many processes take place inside a DSSC. However, two involve the redox couple contained in the electrolyte solution: the dye regeneration and the recombination processes (i.e., the electron transfer from the TiO_2 to the couple or even back to the dye). While the first is a desired path, the latter impacts the power conversion efficiency (PCE) of the DSSC, decreasing the measured values.

This work used different experimental conditions, such as cell configurations and electrode materials, to understand the thermodynamics of the two-electron processes mentioned above. With a sandwich configuration, a DSSC comprises an FTO/TiO_2 photoanode, a counter electrode made of FTO, and a catalytic material. For this reason, the iodine-related couples were evaluated using both electrode materials.

3.1 Cyclic voltammetric studies

The evaluation of 1 mM iodide solutions in the supporting electrolyte (0.1 M $NaClO_4$ aqueous or 0.04 M $C_4H_{12}NClO_4$ in acetonitrile) were performed under different experimental conditions

TABLE 1 Main anodic (E_{an}) and cathodic (E_{cat}) intensity current peaks, a-obtained from different applied routines in 1 mM KI solutions in the supporting electrolyte (0.1 M $NaClO_4$) using a conventional 3-electrodes disposition (conic) (upper part); b-obtained from different applied routines in 1 mM KI solutions in the supporting electrolyte (0.04 M $C_4H_{12}NClO_4$ in acetonitrile) (lower part). Related anodic and cathodic peaks are listed in the same line.

Electrolyte	Au-*pc*		FTO/TiO_2		Reported couples	Number
	E_{an}/V	E_{cat}/V	E_{an}/V	E_{cat}/V		
0.1 M $NaClO_4$ (aqueous)		−0.11		−0.21	$I_3^-/I_2^{\cdot-}$	I
	0.73	0.70			I_3^-/I^- or I_3^-/I_2	III
	1.16	1.11			$I_2^{\cdot-}/I^-$	IV
	1.53				$I^{\cdot}/I^-$ or $IO_3^-/I_{(ad)}$	V
	1.58		1.57			
			2.21		IO/IO^-	VI
acetonitrile				−0.06	$I_3^-/I_2^{\cdot-}$	I
		0.37			$I_2/I_2^{\cdot-}$	II
	0.60				I_3^-/I^-, or I_3^-/I_2	III
	0.91	0.73				
	1.09	0.96			$I_2^{\cdot-}/I^-$	IV
			1.31		$I^{\cdot}/I^-$	V
			1.88		IO/IO^-	VI

and using Au-*pc*, FTO or ITO and FTO/TiO_2 electrodes. Different routines and types of electrochemical cells were applied (*i.e.*, conic in a conventional 3-electrodes disposition, screen-printed traditional drop-mode, SPD, and screen-printed under thin-layer mode, SPTL). The main experimental data obtained from the voltammetric profiles are displayed in Table 1, and displayed in Figures 1, 2.

Voltammetric profiles displayed in Figures 1, 2 showed the presence of several anodic and cathodic contributions, where the reasonable assignation to the iodine-based couples was made according to the literature (Kolthoff and Coetzee, 1957; Rodriguez and Soriaga, 1988; Boschloo and Hagfeldt, 2009). It is essential to clarify that data from the literature are not always coincident, so the measured redox couples and intensity current peaks were assigned considering this dispersion in the reported data. Nevertheless, this situation didn`t affect our calculations and thermodynamics considerations.

Working with a traditional 3-electrode configuration in a conic cell, observing and identifying two reversible redox couples, among other intensity current contributions, was possible (Figures 1, 2). When working with screen-printed electrodes (SPD), the separation between the anodic and the related cathodic counter peak increased. Additionally, an essential improvement in the peak definition was observed when working with screen-printed electrodes but adopting a sandwich configuration (SPTL). The redox couples and the anodic and cathodic contributions were assigned to the reported iodine-based couples as shown in Table 1.

The electrode material is an essential point to consider. Most reported cases of iodine-containing couples are detected using a catalytic material such as gold. However, using FTO or FTO/TiO_2 electrodes, only a few redox reactions were detected. Are these differences relevant? It could be, considering the DSSC constitution. The counter electrode of the DSSC offers a surface where many iodide-related species can be generated and, therefore, are available for the oxidized form of the dye (D^+). Then, the D^+ would have many ways of recovering the lost electrons. Besides, only some of the iodine species are available on the titania surface to allow recombination. The thermodynamics of the processes will be further discussed in Section 3.2.

Voltammetric analyses of two of the most utilized iodine-based electrolytes were also performed (Figures 3, 4). In this case, 1 mM iodide-containing solutions were evaluated. Almost the same features as those observed when working with pure iodide salts were observed, as observed in Table 2. However, fewer redox couples involving iodine species are detected, and redox potential values are lower. As discussed in the following section, this does not affect the thermodynamic considerations associated with the DSSC operation.

3.2 Thermodynamics of the dye regeneration and the recombination processes

When the sunlight inside the DSSC surface, the following processes occur (Nazeeruddin et al., 2011):

$$D + h\nu \rightarrow D^* \quad (1)$$

$$D^* + TiO_2 \rightarrow e(TiO_2) + D^+ \quad (2)$$

Then, under the influence of the light, and as shown in Equations 1, 2, two species are generated: an oxidized form of the dye (with avidity to recover the lost electrons) and an enriched titania (with available electrons to further transferences). At this point, the electrons can be transferred from the titania to the FTO following the desired path for a working DSSC, or the electrons can be transferred to the redox couple of the electrolyte or even back to the oxidized form of the dye. The latter are known as recombination

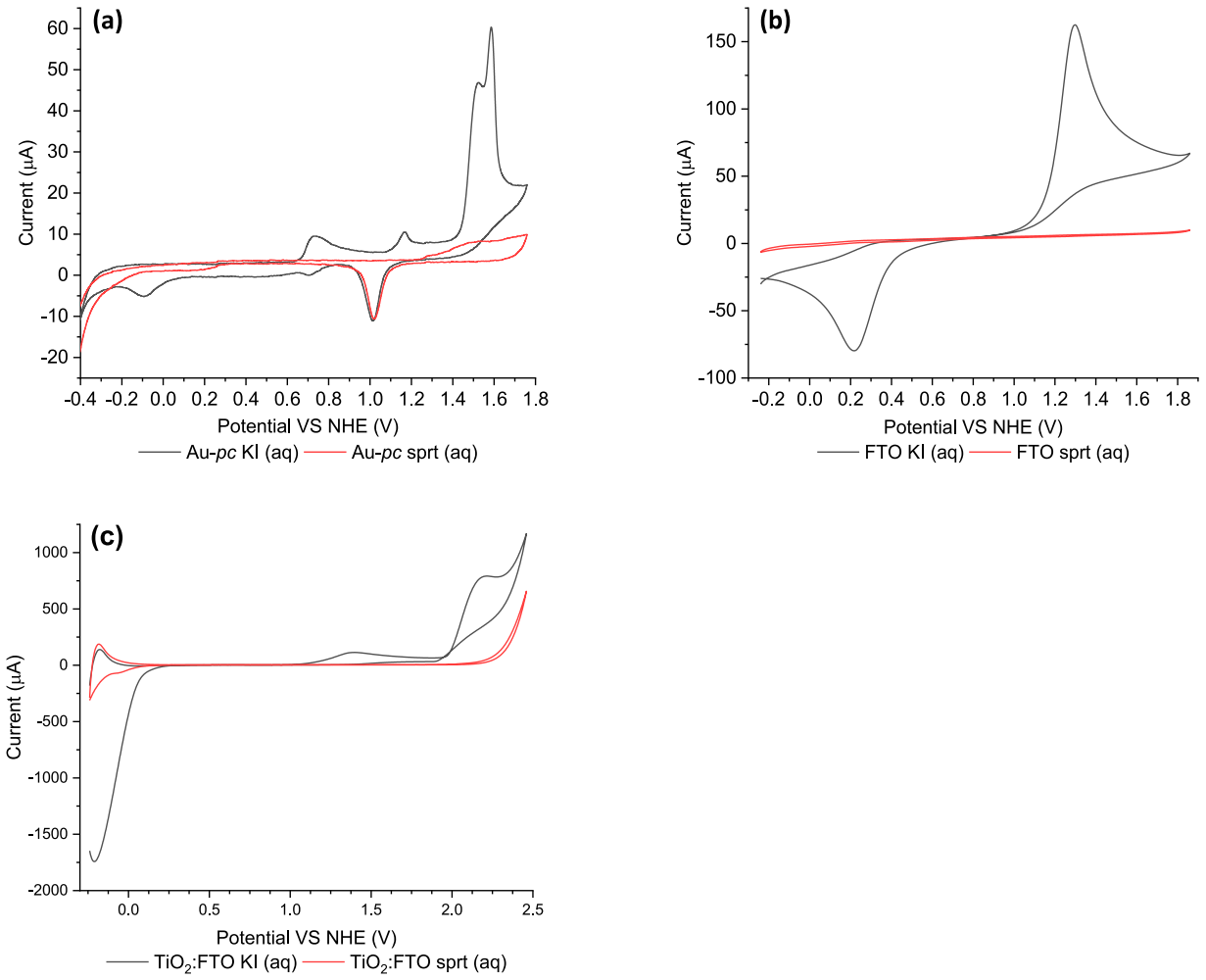

FIGURE 1
Cyclic voltammetric profiles recorded in 1 mM KI in aqueous media solutions (supporting electrolyte 0.1 M $NaClO_4$) performed in a one-compartment conic cell, measured using as working electrodes **(A)** Au-*pc*, **(B)** FTO and **(C)** TiO_2/FTO. v = 0.050 Vs^{-1}. Black lines: 1 mM KI solutions, red lines: supporting electrolyte (sprt).

processes, and due to their existence, the PCE of the DSSC is affected and, thus, lowered. The redox couple dissolved in the electrolyte (typically iodide/triiodide, I^-/I_3^-) must reduce the oxidized dye to regenerate the resting dye. During DSSC operation, the kinetics of dye regeneration must occur rapidly to minimize undesirable charge recombination between the hole state of the D^+ and the electron state in the conduction band of TiO_2.

From an energetic point of view, the potential of the cell reaction composed of an oxidation and a reduction pair has to be positive to ensure the electron transfer between the involved pairs.

For the regeneration of the dye (reg), we can consider many options, considering the generated species onto a catalytic material as the electrode surface of the counter electrode of the DSSC.

The energetic balance, in this case, can be expressed as follows as shown in Equation 3 (Bard and Faulkner, 2000):

$$E_{reg} = E_{dye} - E_{couple} \quad (3)$$

Where the D^+ receives the electrons transferred by the iodine couples.

From all the dyes reported in the literature as suitable sensitizers, only those from natural resources previously evaluated for our group will be considered (Table 3) (Cerdá, 2022; Montagni et al., 2024).

When Equation 3 is applied for an average value of 1.3 V:

$$E_{reg} = 1.30 - E_{couple}$$

In this situation, the dye behaves as an oxidant and, therefore, is reduced, and the iodine-based couple gives the electrons to the dye. Considering the measured cathodic potentials in Table 1, a calculated positive value for the E_{total} (referring to the balance between the redox potential of the pair containing the molecule that is oxidized and the potential of the pair with the species that is reduced) is obtained for all iodine redox couples from II to IV. Then, undoubtedly, the dye could be regenerated considering the existence of a catalytic surface inside the DSSC, allowing the formation of the couples.

$$E_{reg} = 1.30 - E_{couple_{cathodic}}\ (II) = 1.30 - 0.37 = 0.93\,V$$
$$E_{reg} = 1.30 - E_{couple_{cathodic}}\ (III) = 1.30 - 0.73 = 0.57\,V$$

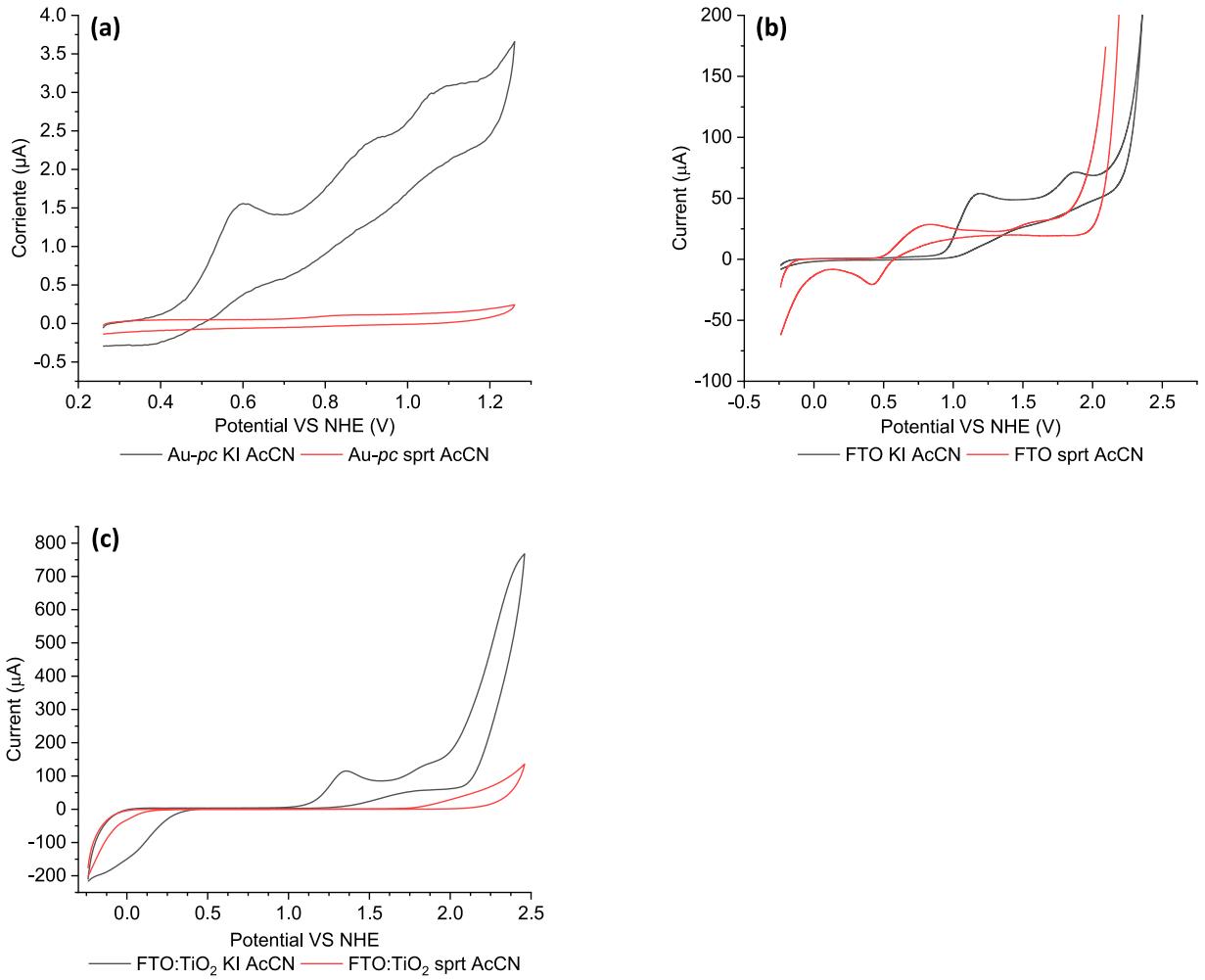

FIGURE 2
Cyclic voltammetric profiles recorded in 1 mM KI in acetonitrile solutions (supporting electrolyte 0.04 M $C_4H_{12}NClO_4$) performed in a one-compartment conic cell, measured using as working electrodes **(A)** Au-*pc*, **(B)** FTO and **(C)** TiO_2/FTO. v = 0.050 Vs^{-1}. Black lines: 1 mM KI solutions, red lines: supporting electrolyte (sprt).

$$E_{reg} = 1.30 - E_{couple_{cathodic}}\ (IV) = 1.30 - 0.96 = 0.34\,V$$

The involved reactions would be:
For the dye (Equation 4):

$$D^+ + e^- \rightarrow D \tag{4}$$

While for the iodine-based couples (Equations 5–8):

$$I_2^{-\cdot} \rightarrow I_2 + 2e^- \tag{5}$$

$$3I^- \rightarrow I_3^- + 2e^- \tag{6}$$

$$2I_3^- \rightarrow 3I_2 + 2e^- \tag{7}$$

$$2I^- \rightarrow I_2^{-\cdot} + 2e^- \tag{8}$$

A different situation occurs on the FTO/TiO_2 surface. After the dye adsorption, many spots on the semiconductor surface remain uncovered or naked. This means that iodine species can reach these naked spots and receive electrons from the titania in the recombination (recomb) process. In this case, the balance will be as shown in Equation 9:

$$E_{recomb} = E_{couple} - E_{titania} \tag{9}$$

Less electron exchange processes could occur because, as shown in Table 1, this surface is less reactive than gold or platinum surfaces.

In this situation, for a reported $E_{titania}$ value of −0.53 V (Kalyanasundaram and Grätzel, 1998) and considering reactions V and VI, measured on the FTO/TiO_2 surface, Equation 9 is:

$$E_{recomb} = E_{couple_{anodic}}\ (V) - E_{titania} = 1.31 + 0.53 = 1.84\,V$$

$$E_{recomb} = E_{couple_{anodic}}\ (VI) - E_{titania} = 1.88 + 0.53 = 2.41\,V$$

In this case, the semi reaction for the titania would be, according to Equation 10:

$$e\,(TiO_2) \rightarrow TiO_2 + e^- \tag{10}$$

While for the iodine-based couples Equations 11, 12 could be applied:

$$I^{\cdot} + e^- \rightarrow I^- \tag{11}$$

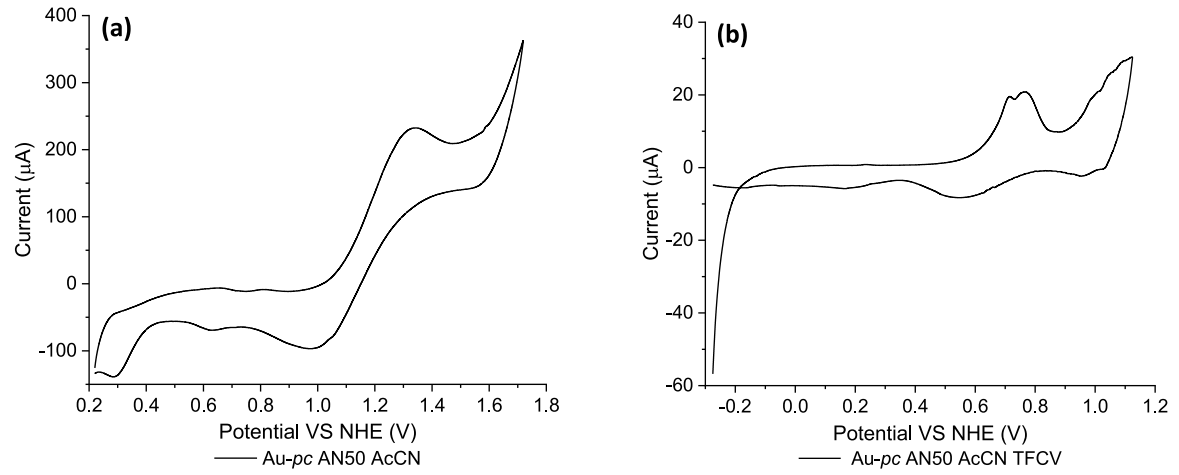

FIGURE 3
Cyclic voltammetric profiles of Au-*pc* recorded in Iodolyte AN50 electrolyte diluted in acetonitrile (final iodide estimated concentration 1 mM) using two different cells configuration: **(A)** SPD (screen-printed electrodes inside a conic cell), v = 0.050 Vs^{-1}, and **(B)** SPTL (screen-printed electrodes following a thin-film configuration), v = 0.010 Vs^{-1}.

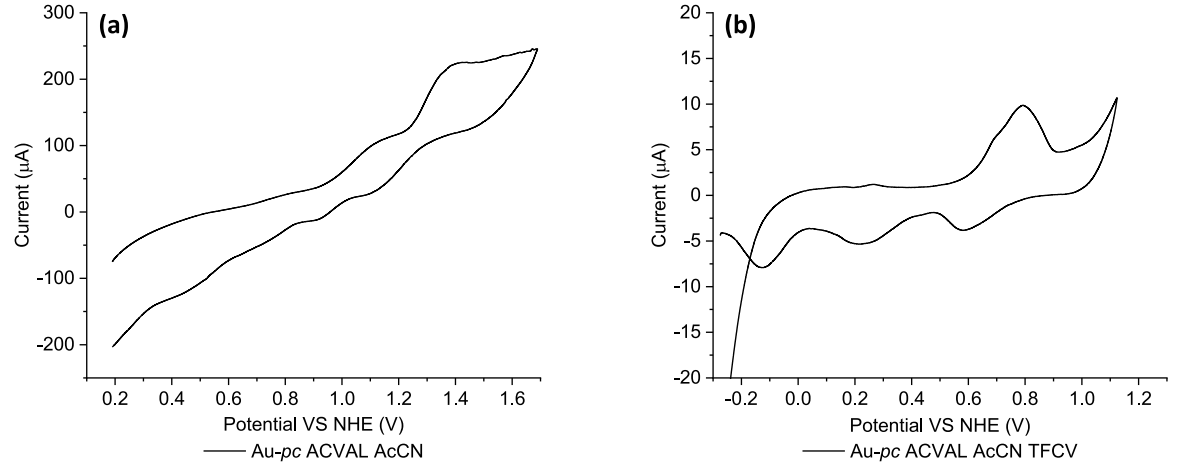

FIGURE 4
Cyclic voltammetric profiles of Au-*pc* recorded in the ACVAL electrolyte diluted in acetonitrile (final iodide estimated concentration 1 mM) using two different cells configuration: **(A)** SPD (screen-printed electrodes inside a conic cell), v = 0.050 Vs^{-1}, and **(B)** SPTL (screen-printed electrodes following a thin-film configuration), v = 0.010 Vs^{-1}.

$$IO + e^- \rightarrow IO^- \quad (12)$$

In the present circumstance, the recombination process is thermodynamically favoured. Thus, the $e(TiO_2)$ can transfer the electrons directly to the redox couple instead of transferring the electrons to the FTO. As a consequence, the PCE of the DSSC is affected and decreases.

Also, recombination can be explained by the electron transfer between $e(TiO_2)$ and the oxidized dye. In the above situation, titania acts as the reducing agent and D^+ as the oxidant. Here, the thermodynamics of this electron exchange can be written as:

$$E_{recomb} = E_{dye} - E_{titania}$$
$$E_{recomb} = 1.30 + 0.53 = 1.83\,V$$

Once again, the recombination reaction involving the back transfer from the titania could take place. The semi-reactions would be:

For the dye (Equation 4):

$$D^+ + e^- \rightarrow D$$

And for the titania (Equation 10):

$$e(TiO_2) \rightarrow TiO_2 + e^-$$

Similar calculations can be carried out considering the electrolytes most used in DSSC. Even when redox-measured couples are not the same as those detected with KI, the potential difference between the dye oxidation potential and the electrolytes reduction potential shows that

TABLE 2 Main anodic (E_{an}) and cathodic (E_{cat}) intensity current peaks, obtained either from conventional conic cell three-electrode system cyclic voltammetry (left) or screen-printed thin-film cyclic voltammetry (right) using commercial Solaronix Iodolyte AN50 (upper part) or ACVAL electrolyte (lower part).

Electrolyte	Au-*pc*/conic (		Au-*pc*/SPTL		Reported couples	Number
	E_{an}/V	E_{cat}/V	E_{an}/V	E_{cat}/V		
AN50				0.16	$I_3^-/I_2^{\cdot-}$	I
	0.31	0.29			$I_2/I_2^{\cdot-}$	II
	0.65	0.63	0.72	0.55	I_3^-/I^-, or I_3^-/I_2	III
	0.81		0.77			
		0.96	1.01	0.95	$I_2^{\cdot-}/I^-$	IV
			1.05			
	1.33				$I^{\cdot}/I^-$	V
ACVAL				−0.12	$I_3^-/I_2^{\cdot-}I^-$	I
	0.48	0.45	0.27	0.23	$I_2/I_2^{\cdot-}$ or I_3^-/I^-	II
				0.58	I_3^-/I^- or I_3^-/I_2	III
			0.70			
	0.83		0.79		$I_2^{\cdot-}/I^-$	IV
	1.10	1.11			$I_2^{\cdot-}/I^-$	IV
	1.39				$I^{\cdot}/I^-$	V

TABLE 3 Potential peak values for the main anodic intensity current peaks reported for the most abundant natural dyes (Cerdá, 2022).

Dye	E_{anodic}/V vs. NHE
anthocyanins	1.30
carotenoids	1.40
phycobiliproteins	1.40
violacein	1.20

the regeneration process is still possible and occurs inside an assembled cell (Reactions I to IV in Table 2). Then, for AN50 and ACVAL Equation 3 could be written as:

$$E_{reg} = 1.30 - E_{couple_{cathodic}}\ (I) = 1.30 - 0.16 = 1.14\,V$$
$$E_{reg} = 1.30 - E_{couple_{cathodic}}\ (II) = 1.30 - 0.23 = 1.07\,V$$
$$E_{reg} = 1.30 - E_{couple_{cathodic}}\ (III) = 1.30 - 0.58 = 0.72\,V$$
$$E_{reg} = 1.30 - E_{couple_{cathodic}}\ (IV) = 1.30 - 0.95 = 0.35\,V$$

As cathodic measured potentials are lower than 1 V, the regeneration will be positive and, therefore, thermodynamically possible.

Following analogue reasoning, one can argue that the recombination process is thermodynamically feasible whenever the electrolyte (AN50 as well as ACVAL) has an oxidation potential greater than the titania Fermi level, which (within the experimental conditions of this work) are all of the anodic potentials measured (II to IV according to Table 2). With the previous statement in mind, the E_{recomb} of the electrolyte (considering couples II to IV), will be positive, and Equation 9 could be written as:

$$E_{recomb} = E_{couple_{anodic}}\ (II) - E_{titania} = 0.27 + 0.53 = 0.80\,V$$
$$E_{recomb} = E_{couple_{anodic}}\ (III) - E_{titania} = 0.70 + 0.53 = 1.23\,V$$
$$E_{recomb} = E_{couple_{anodic}}\ (IV) - E_{titania} = 0.79 + 0.53 = 1.32\,V$$

Figure 5 summarizes the above-discussed results. It shows a redox potential diagram depicting the energy levels of the dye, the TiO_2, and all iodine species measured (against NHE) in this work.

3.3 Kinetics of the main processes involved in a DSSC

Exploring the thermodynamic calculations helps understand the main electron exchange processes inside a DSSC, where the balance between regeneration and recombination directly affects the cell's overall performance. Additionally, it allows the comprehension of the thermodynamically possible processes and which couples could be involved. However, thermodynamics is not enough; evaluating the kinetics of the involved main processes is necessary. Then, using electrochemical impedance spectroscopy (EIS) measurements, it is possible to calculate the recombination and the electron transfer times.

Analyzing the experimental data measured by EIS reveals the importance of high recombination times and time constants. Recombination mainly involves the injection of electrons from the semiconductor into the liquid electrolyte containing the redox couples. This process, where the electrons generated after the light reaches the pigment's surface, followed an undesired path, resulting in decreased power conversion efficiency. On the other hand, the time constant is about the transport of the injected electrons diffusing through the semiconductor network.

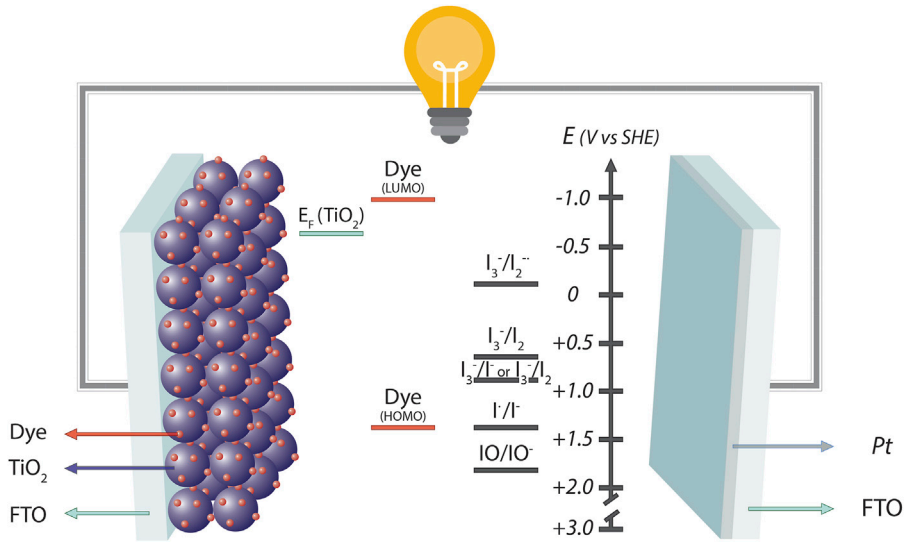

FIGURE 5
Redox potential diagram, depicting the energy levels of the dye, the TiO_2 and all iodine species measured (against NHE) in this work. In these diagrams, the energy increases, as pointed out in the arrow above (opposite to the redox potential). In so doing, the thermodynamically most favorable path towards an energy minimum for the electron will be taken downstream.

TABLE 4 Values obtained from fitting the experimental data measured at V = 0.5 V, in darkness, using a transmission line based model. Γt = the time constant for the transport of the injected electrons that diffuse through the nanoparticle network (calculated as Γt = Rt × Cμ, with Cμ, the chemical capacitance at the TiO_2/dye/electrolyte interface, associated with the variation in the electron density and the displacement of the Fermi level and Rt is the electron transport resistance to the photoanode); Γrec = the recombination time that reflects the lifetime of an electron in the photoanode (calculated as Γrec = Rct × Cμ, where Rct is the charge transference resistance).

Dye	Main compound	$\Gamma_{rec} = R_{ct} \times C_\mu$/s	$\Gamma_t = R_t \times C_\mu$/s	Reference
anthocyanins	cyanidin 3-O-glucoside	0.0840	0.00180	Enciso et al. (2017)
	delphinidin-3-glucoside	0.1300	0.00077	Montagni et al. (2023)
carotenoids	β,β-Carotene	0.0060	0.00180	Montagni et al. (2024)
	myxoxanthophyll-like derivates	0.0300	0.00100	Montagni et al. (2024)
	fucoxanthin	0.0370	0.00140	de Bon et al. (2022)
proteins	phycoerythrin	0.0900	0.00300	Cerdá and Botasini (2020)
bacterial	violacein	0.1700	0.00400	Marizcurrena et al. (2021)

The performances of the measured DSSC are affected by the balance between the recombination times and the time constants (and, therefore, between the Rct and Rt resistances). When generated, electrons can follow transference across the semiconductor or recombine with the electrolyte. The ratio between the Γrec and the Γt helps us understand the efficiency values. The calculated data values for the time constants are similar for the different natural dyes used as sensitizers (Table 4). Considering the data previously analyzed by our group results from DSSC devices sensitized with natural dyes showed no significant differences. They also showed reasonable ratios Γrec to Γt, which means that recombination times are larger than transport ones. And calculated ratios are also very similar. This is in line with thermodynamics calculations displayed in this work. Cells sensitized with natural dyes show different power conversion efficiencies, depending on the selected type of dye, but they do not differ so much. The efficiencies of DSSC with natural dyes are much lower than those containing synthesized dyes. For synthetic dyes, the time constants are not so different from the values reported for the natural ones, but differences are raised from the recombination time's values, which are primarily around one second or even more (Gao et al., 2008; Cao et al., 2009; Yum et al., 2012; Yum et al., 2013; Yang et al., 2014). Then, when recombination is retarded, it is possible to obtain a highly efficient DSSC.

3.4 Final remaks

The thermodynamics analysis involved the different redox couples from the electrolytes applied to assemble the DSSC, as

TABLE 5 Photovoltaic properties of cells assembled with different sensitizers. All measurements were performed under one sun light intensity of 100 mWcm^{-2}, AM 1.5G. Jsc is the short-circuit current density, Voc the open circuit potential, and η is the power conversion efficiency (PCE). Average values coming from at least three independent assembled cells.

Dye		Jsc/mA cm^{-2}	Voc/V	η/%	Reference
anthocyanins	Cyaniding 3-O-glucoside	2.63	0.50	0.730	Enciso et al. (2017)
	delphinidin-3-glucoside	0.51	0.50	0.170	Montagni et al. (2023)
carotenoids	β,β-Carotene	1.9×10^{-4}	0.48	0.048	Montagni et al. (2024)
	myxoxanthophyll-like derivates	3.4×10^{-4}	0.56	0.127	Montagni et al. (2024)
	fucoxanthin	0.38	0.53	0.120	de Bon et al. (2022)
protein	phycoerythrin	3.8×10^{-4}	0.61	0.126	Cerdá and Botasini (2020)
bacterial	violacein	5.2×10^{-4}	0.55	0.170	Marizcurrena et al. (2021)

well as the redox behaviour of the dyes and the titania itself. According to our calculations, many processes can take place inside the cells, but some are of particular relevance: 1- dye regeneration, 2- electron recombination from the titania to the redox couples contained in the electrolyte, and 3- electron transport or time constants across the semiconductor network.

The thermodynamics and the kinetics treatment previously displayed are consistent with a prevalence of electron recombination, especially for DSSC sensitized with natural dyes.

Experimental data confirmed this statement, as observed for the Jsc and the power conversion efficiency values previously reported for our group (Table 5).

4 Conclusion

DSSCs are composed of two electrodes: one containing a catalytic material and the other containing the dye adsorbed to a semiconductor, leaving blank naked spots on the TiO_2 surface. A liquid electrolyte (primarily based on iodine-related species) is placed in between, especially when working with natural dyes. Among all the electronic exchange processes inside the DSSC, those related to dye regeneration and electron transfer from the titania are the most relevant, with a clear incidence in the performance of the assembled cell.

Our results show that different iodine-based redox couples are involved, considering the different electrode surfaces inside the DSSC. Consequently, different redox couples can be considered: some iodine species evolved onto a catalytic surface and others onto the semiconductor. Then, redox couples involved in the dye's regeneration are not the same as in the recombination processes. The present work shows that both processes are thermodynamically possible, but, unfortunately, the recombination (the electron transfer from the titania to the redox couple or even back to the dye instead of towards the FTO surface) is predominant over the regeneration of the dye. These results are in agreement with kinetic data, arising from EIS and also with current density and potential profiles, previously reported by our group.

Data availability statement

The raw data supporting the conclusions of this article will be made available by the authors, without undue reservation.

Author contributions

MA: Formal Analysis, Writing–review and editing, Investigation, Software. MFC: Conceptualization, Formal Analysis, Methodology, Supervision, Writing–original draft, Writing–review and editing.

Funding

The author(s) declare that no financial support was received for the research, authorship, and/or publication of this article.

Acknowledgments

María Fernanda Cerdá is a SNI-ANII (Agencia Nacional de Investigación e Innovación) and PEDECIBA (Programa de Desarrollo de las Ciencias Básicas) researcher.

Conflict of interest

The authors declare that the research was conducted in the absence of any commercial or financial relationships that could be construed as a potential conflict of interest.

Generative AI statement

The author(s) declare that no Generative AI was used in the creation of this manuscript.

Publisher's note

References

Alhamed, M., Issa, A. S., and Doubal, A. W. (2012). Studying of natural dyes properties as photo-sensitizer for dye sensitized solar cells (DSSC). *J. Electron Devices* 16 (11), 1370–1383.

Arifin, Z., Soeparman, S., Widhiyanuriyawan, D., and Suyitno, S. (2017). Performance enhancement of dye-sensitized solar cells using a natural sensitizer. *Int. J. Photoenergy* 2017, 1–5. doi:10.1155/2017/2704864

Aslam, A., Mehmood, U., Arshad, M. H., Ishfaq, A., Zaheer, J., Ul Haq Khan, A., et al. (2020). Dye-sensitized solar cells (DSSCs) as a potential photovoltaic technology for the self-powered internet of things (IoTs) applications. *Sol. Energy* 207, 874–892. doi:10.1016/j.solener.2020.07.029

Ates, M., Karazehir, T., and Uludag, N. (2012). Electrolyte effects of poly(3-methylthiophene) via PET/ITO and synthesis of 5-(3,6-di(thiophene-2-yl)-9H-carbazole-9-yl) pentanitrile on electrochemical impedance spectroscopy. *J. Appl. Polym. Sci.* 125 (4), 3302–3312. doi:10.1002/app.36581

Baby, R., Nixon, P. D., Kumar, N. M., Subathra, M. S. P., and Ananthi, N. (2022). A comprehensive review of dye-sensitized solar cell optimal fabrication conditions, natural dye selection, and application-based future perspectives. *Environ. Sci. Pollut. Res.* 29, 371–404. doi:10.1007/s11356-021-16976-8

Bard, A. J., and Faulkner, L. R. (2000). *Electrochemical methods: fundamentals and applications*. 2nd Edition. New Jersey: John Wiley and Sons, Inc.

Barichello, J., Mariani, P., Vesce, L., Spadaro, D., Citro, I., Matteocci, F., et al. (2024). Bifacial dye-sensitized solar cells for indoor and outdoor renewable energy-based application. *J. Mater. Chem. C* 12, 2317–2349. doi:10.1039/D3TC03220E

Basheer, B., Mathew, D., George, B. K., and Reghunadhan Nair, C. (2014). An overview on the spectrum of sensitizers: the heart of Dye Sensitized Solar Cells. *Sol. Energy* 108, 479–507. doi:10.1016/j.solener.2014.08.002

Baucke, F. G. K., Bertram, R., and Cruse, K. (1971). The iodide-iodine system in acetonitrile: evaluation of standard thermodynamic data on the association I−+I2→I3− from potentiometric measurements at 25 and 50°C. *J. Electroanal. Chem. Interfacial Electrochem.* 32 (2), 247–256. doi:10.1016/S0022-0728(71)80190-0

Bisquert, J., Cahen, D., Hodes, G., Rühle, S., and Zaban, A. (2004). Physical chemical principles of photovoltaic conversion with nanoparticulate, mesoporous dye-sensitized solar cells. *J. Phys. Chem. B* 108, 8106–8118. doi:10.1021/jp0359283

Boschloo, G. (2019). Improving the performance of dye-sensitized solar cells. *Front. Chem.* 7, 77. doi:10.3389/fchem.2019.00077

Boschloo, G., Gibson, E. A., and Hagfeldt, A. (2011). Photomodulated voltammetry of iodide/triiodide redox electrolytes and its relevance to dye-sensitized solar cells. *J. Phys. Chem. Lett.* 2 (24), 3016–3020. doi:10.1021/jz2014314

Boschloo, G., and Hagfeldt, A. (2009). Characteristics of the iodide/triiodide redox mediator in dye-sensitized solar cells. *Accounts Chem. Res.* 42 (11), 1819–1826. doi:10.1021/ar900138m

Botasini, S., Martí, A. C., and Méndez, E. (2016). Thin-layer voltammetry of soluble species on screen-printed electrodes: proof of concept. *Analyst* 141, 5996–6001. doi:10.1039/C6AN01374K

Cao, Y., Bai, Y., Yu, Q., Cheng, Y., Liu, S., Shi, D., et al. (2009). Dye-sensitized solar cells with a high absorptivity ruthenium sensitizer featuring a 2-(hexylthio)thiophene conjugated bipyridine. *J. Phys. Chem. C* 113 (15), 6290–6297. doi:10.1021/jp9006872

Cerdá, M. F. (2022). Dyes from the southern lands: an alternative or a dream? *Solar* 2, 519–539. doi:10.3390/solar2040031

Cerdá, M. F., and Botasini, S. (2020). Co-sensitized cells from Antarctic resources using Ag nanoparticles. *Surf. Interface Analysis* 52, 980–984. doi:10.1002/sia.6849

Chandra Sil, M., Chen, L. S., Lai, C. W., Lee, Y. H., Chang, C. C., and Chen, C. M. (2020). Enhancement of power conversion efficiency of dye-sensitized solar cells for indoor applications by using a highly responsive organic dye and tailoring the thickness of photoactive layer. *J. Power Sources* 479, 229095. doi:10.1016/j.jpowsour.2020.229095

Daeneke, T., Mozer, A. J., Kwon, T. H., Duffy, N. W., Holmes, A. B., Bach, U., et al. (2012). Dye regeneration and charge recombination in dye-sensitized solar cells with ferrocene derivatives as redox mediators. *Energy and Environ. Sci.* 5, 7090–7099. doi:10.1039/c2ee21257a

Dai, S., Weng, J., Sui, Y., Chen, S., Xiao, S., Huang, Y., et al. (2008). The design and outdoor application of dye-sensitized solar cells. *Inorganica Chim. Acta* 361 (3), 786–791. doi:10.1016/j.ica.2007.04.018

Dané, L. M., Janssen, L. J. J., and Hoogland, J. G. (1968). The iodine/iodide redox couple at a platinum electrode. *Electrochimica Acta* 13 (3), 507–518. doi:10.1016/0013-4686(68)87022-7

de Bon, M., Rodríguez Chialanza, M., and Cerdá, M. F. (2022). Fucoxanthin from the antarctic himantothallus grandifollius as a sensitizer in DSSC. *J. Iran. Chem. Soc.* 19, 3627–3636. doi:10.1007/s13738-022-02560-5

Devadiga, D., Selvakumar, M. Y., Shetty, P., and Santosh, M. S. (2021). Dye-sensitized solar cell for indoor applications: a mini-review. *J. Electron. Mater.* 50, 3187–3206. doi:10.1007/s11664-021-08854-3

Dhonde, M., Sahu, K., Das, M., Yadav, A., Ghosh, P., and Murty, V. V. S. (2022). Review—recent advancements in dye-sensitized solar cells; from photoelectrode to counter electrode. *J. Electrochem. Soc.* 169 (6), 066507. doi:10.1149/1945-7111/ac741f

Enciso, P., Decoppet, J. D., Grätzel, M., Wörner, M., Cabrerizo, F. M., and Cerdá, M. F. (2017). A cockspur for the DSS cells: *Erythrina crista-galli* sensitizers. *Spectrochimica Acta Part A Mol. Biomol. Spectrosc.* 176, 91–98. doi:10.1016/j.saa.2017.01.002

Ferdowsi, P., Saygili, Y., Jazaeri, F., Edvinsson, T., Mokhtari, J., Zakeeruddin, S. M., et al. (2020). Molecular engineering of simple metal-free organic dyes derived from triphenylamine for dye-sensitized solar cell applications. *ChemSusChem* 13, 212–220. doi:10.1002/cssc.201902245

Francis, O. I., and Ikenna, A. (2021). Review of dye-sensitized solar cell (DSSCs) development. *Nat. Sci.* 13 (12), 496–509. doi:10.4236/ns.2021.1312043

Gao, F., Wang, Y., Shi, D., Zhang, J., Wang, M., Jing, X., et al. (2008). Enhance the optical absorptivity of nanocrystalline TiO2 film with high molar extinction coefficient ruthenium sensitizers for high performance dye-sensitized solar cells. *J. Am. Chem. Soc.* 130 (32), 10720–10728. doi:10.1021/ja801942j

García-Miranda Ferrari, A., Rowley-Neale, S. J., and Banks, C. E. (2021). Screen-printed electrodes: transitioning the laboratory in-to-the field. *Talanta Open* 3, 100032. doi:10.1016/j.talo.2021.100032

Hamed, N. K. A., Ahmad, M. K., Urus, N. S. T., Mohamad, F., Nafarizal, N., Ahmad, N., et al. (2017). Performance comparison between silicon solar panel and dye-sensitized solar panel in Malaysia. *AIP Conf. Proc.* 1883 (020029), 20029–20037. doi:10.1063/1.5002047

Hubbard, A. T. (1969). Study of the kinetics of electrochemical reactions by thin-layer voltammetry: I. theory. *J. Electroanal. Chem. Interfacial Electrochem.* 22 (2), 165–174. doi:10.1016/S0022-0728(69)80247-0

Hyun, J. Y., Park, B. R., Kim, N. H., and Moon, J. W. (2022). Building energy performance of DSSC BIPV windows in accordance with the lighting control methods and climate zones. *Sol. Energy* 244, 279–288. doi:10.1016/j.solener.2022.08.039

Jasim, K. E. (2011). *Dye sensitized solar cells – working principles, challenges and opportunities*. London, United Kingdom: Solar Cells - Dye-Sensitized Devices, 171–204. doi:10.5772/19749

Jeon, J., Park, Y. C., Han, S. S., Goddard, W. A., III, Lee, Y. S., and Kim, H. (2014). Rapid dye regeneration mechanism of dye-sensitized solar cells. *J. Phys. Chem. Lett.* 5 (24), 4285–4290. doi:10.1021/jz502197b

Jiao, Y., Zhang, F., Meng, S. Y., and Kosyachenko, L. A. (2011). Dye sensitized solar cells principles and new design. *Sol. Cells-Dye-Sensitized Devices* 1 (1). doi:10.5772/21393

Kalyanasundaram, K., and Grätzel, M. (1998). Applications of functionalized transition-metal complexes in photonic and optoelectronic devices. *Coord. Chem. Rev.* 177 (1), 347–414. doi:10.1016/S0010-8545(98)00189-1

Kelíšková, P., Matvieiev, O., Janíková, L., and Šelešovská, R. (2023). Recent advances in the use of screen-printed electrodes in drug analysis: a review. *Curr. Opin. Electrochem.* 42, 101408. doi:10.1016/j.coelec.2023.101408

Khan, M., Iqbal, M. A., Malik, M., Hashmi, S. U., Bakhsh, S., Sohail, M., et al. (2023). Improving the efficiency of dye-sensitized solar cells based on rare-earth metal modified bismuth ferrites. *Sci. Rep.* 13, 3123. doi:10.1038/s41598-023-30000-8

Kolthoff, I. M., and Coetzee, J. F. (1957). Polarography in acetonitrile. II. Metal ions which have significantly different polarographic properties in acetonitrile and in water. Anodic waves. Voltammetry at rotated platinum electrode. *J. Am. Chem. Soc.* 79 (8), 1852–1858. doi:10.1021/ja01565a023

Korir, B. K., Kibet, J. K., and Ngari, S. M. (2024). A review on the current status of dye-sensitized solar cells: toward sustainable energy. *Energy Sci. and Eng.* 12, 3188–3226. doi:10.1002/ese3.1815

Marizcurrena, J. J., Castro-Sowinski, S., and Cerdá, M. F. (2021). Improving the performance of dye-sensitized solar cells using nanoparticles and a dye produced by an Antarctic bacterium. *Environ. Sustain.* 4, 711–721. doi:10.1007/s42398-021-00168-8

Marzouk, S. A. M., Alyammahi, A. R., and Fanjul-Bolado, P. (2021). Development and characterization of novel flow injection, thin-layer, and batch cells for electroanalytical applications using screen-printed electrodes. *Anal. Chem.* 93 (49), 16690–16699. doi:10.1021/acs.analchem.1c04337

Masud, H. K. K. (2023). Redox shuttle-based electrolytes for dye-sensitized solar cells: comprehensive guidance, recent progress, and future perspective. *ACS Omega* 8, 6139–6163. doi:10.1021/acsomega.2c06843

Montagni, T., Ávila, M., Fernández, S., Bonilla, S., and Cerdá, M. F. (2024). Cyanobacterial pigments as natural photosensitizers for dye-sensitized solar cells. *Photochem* 4, 388–403. doi:10.3390/photochem4030024

Montagni, T., Rodríguez Chialanza, M., and Cerdá, M. F. (2023). Blueberries as a source of energy: physical chemistry characterization of their anthocyanins as dye-sensitized solar cells' sensitizers. *Solar* 3 (2), 283–297. doi:10.3390/solar3020017

Morrin, A., Killard, A. J., and Smyth, M. R. (2003). Electrochemical characterization of commercial and home-made screen-printed carbon electrodes. *Anal. Lett.* 36 (9), 2021–2039. doi:10.1081/AL-120023627

Muñoz-García, A. B., Benesperi, I., Boschloo, G., Concepcion, J. J., Delcamp, J. H., Gibson, E. A., et al. (2021). Dye-sensitized solar cells strike back. *Chem. Soc. Rev.* 50, 12450–12550. doi:10.1039/d0cs01336f

Nazeeruddin, Md. K., Baranoff, E., and Grätzel, M. (2011). Dye-sensitized solar cells: a brief overview. *Sol. Energy* 85 (6), 1172–1178. doi:10.1016/j.solener.2011.01.018

O'Regan, B., and Grätzel, M. (1991). A low-cost, high-efficiency solar cell based on dye-sensitized colloidal TiO2 films. *Nature* 353, 737–740. doi:10.1038/353737a0

Popov, A. I., and Deskin, W. A. (1958). Studies on the chemistry of halogens and of polyhalides. XV. Iodine halide complexes with acetonitrile. *J. Am. Chem. Soc.* 80 (12), 2976–2979. doi:10.1021/ja01545a019

Ren, Y., Zhang, D., Suo, J., Cao, Y., Eickemeyer, F. T., Vlachopoulos, N., et al. (2023). Hydroxamic acid pre-adsorption raises the efficiency of cosensitized solar cells. *Nature* 613, 60–65. doi:10.1038/s41586-022-05460-z

Robson, K. C., Bomben, P. G., and Berlinguette, C. P. (2012). Cycloruthenated sensitizers: improving the dye-sensitized solar cell with classical inorganic chemistry principles. *Dalton Trans.* 41 (26), 7814–7829. doi:10.1039/c2dt30825h

Rodriguez, J. F., and Soriaga, M. P. (1988). Reductive desorption of iodine chemisorbed on smooth polycrystalline gold electrodes. *J. Electrochem. Soc.* 135 (3), 616–618. doi:10.1149/1.2095673

Semalti, P., and Sharma, S. N. (2020). Dye sensitized solar cells (DSSCs) electrolytes and natural photo-sensitizers: a review. *J. Nanosci. Nanotechnol.* 20, 3647–3658. doi:10.1166/jnn.2020.17530

Sen, A., Putra, M. H., Biswas, A. K., Behera, A. K., and Groβ, A. (2023). Insight on the choice of sensitizers/dyes for dye sensitized solar cells: a review. *Dyes Pigments* 213, 111087. doi:10.1016/j.dyepig.2023.111087

Shalini, S., Balasundaraprabhu, R., Kumar, T. S., Prabavathy, N., Senthilarasu, S., and Prasanna, S. (2016). Status and outlook of sensitizers/dyes used in dye sensitized solar cells (DSSC): a review. *Int. J. Energy Res.* 40 (10), 1303–1320. doi:10.1002/er.3538

Sharma, K., Sharma, V. Y., and Sharma, S. S. (2018). Dye-sensitized solar cells: fundamentals and current status. *Nanoscale Res. Lett.* 13 (381), 1–46. doi:10.1186/s11671-018-2760-6

Spadaro, D., Tropea, A., Citro, I., Trocino, S., Giuffrida, D., Rigano, F., et al. (2024). Development of innovative dye sensitized solar cells (DSSCs) based on co-sensitization of natural microbial pigments. *Dyes Pigments* 229, 112311. doi:10.1016/j.dyepig.2024.112311

Stanbury, D. M. (1989). "Reduction potentials involving inorganic free radicals in aqueous solution," in *Advances in inorganic chemistry*. Editor A. G. Sykes (Academic Press), 33, 69–138. doi:10.1016/S0898-8838(08)60194-4

Stanbury, D. M., Wilmarth, W. K., Khalaf, S., Po, H. N., and Byrd, J. E. (1980). Oxidation of thiocyanate and iodide by iridium(IV). *Inorg. Chem.* 19 (9), 2715–2722. doi:10.1021/ic50211a046

Sun, Z., Liang, M., and Chen, J. (2015). Kinetics of iodine-free redox shuttles in dye-sensitized solar cells: interfacial recombination and dye regeneration. *Accounts Chem. Res.* 48 (6), 1541–1550. doi:10.1021/ar500337g

Tanner, E., and Compton, R. (2018). How can electrode surface modification benefit electroanalysis? *Electroanalysis* 30, 1336–1341. doi:10.1002/elan.201700807

Uludag, N., Yarapsanlı, Y., Asutay, O., and Gumus, M. K. (2018). 'Cycloaddition of enamines with 1,4-Dimethoxy-2-butyne and 2-Butyne-1,4-diol mediated by titanium tetrachloride. *Org. Prep. Proced. Int.* 50 (4), 441–448. doi:10.1080/00304948.2018.1468987

Wang, X., and Stanbury, D. M. (2006). Oxidation of iodide by a series of Fe(III) complexes in acetonitrile. *Inorg. Chem.* 45 (9), 3415–3423. doi:10.1021/ic052022y

Wang, X., Zhang, Z., Wu, G., Xu, C., Wu, J., Zhang, X., et al. (2022). Applications of electrochemical biosensors based on functional antibody-modified screen-printed electrodes: a review. *Anal. Methods* 14, 7–16. doi:10.1039/D1AY01570B

Yanagida, S., Yu, Y., and Manseki, K. (2009). Iodine/iodide-free dye-sensitized solar cells. *Accounts Chem. Res.* 42 (11), 1827–1838. doi:10.1021/ar900069p

Yang, J., Ganesan, P., Teuscher, J., Moehl, T., Kim, Y. J., Yi, C., et al. (2014). Influence of the donor size in D–π–A organic dyes for dye sensitized solar cells. *J. Am. Chem. Soc.* 136, 5722–5730. doi:10.1021/ja500280r

Yum, J. H., Baranoff, E., Kessler, F., Moehl, T., Ahmad, S., Bessho, T., et al. (2012). A cobalt complex redox shuttle for dye-sensitized solar cells with high open-circuit potentials. *Nat. Commun.* 3 (631), 631. doi:10.1038/ncomms1655

Yum, J. H., Holcombe, T. W., Kim, Y., Rakstys, K., Moehl, T., Teuscher, J., et al. (2013). Blue-coloured highly efficient dye- sensitized solar cells by implementing the diketopyrrolopyrrole chromophore. *Sci. Rep.* 3 (2446), 2446. doi:10.1038/srep02446

Zhang, D., Stojanovic, M., Ren, Y., Cao, Y., Eickemeyer, F. T., Socie, E., et al. (2021). A molecular photosensitizer achieves a Voc of 1.24 V enabling highly efficient and stable dye-sensitized solar cells with copper(II/I)-based electrolyte. *Nat. Commun.* 12, 1777. doi:10.1038/s41467-021-21945-3

Zhou, W., Liu, W., Qin, M., Chen, Z., Xu, J., Cao, J., et al. (2020). Fundamental properties of TEMPO-based catholytes for aqueous redox flow batteries: effects of substituent groups and electrolytes on electrochemical properties, solubilities and battery performance. *RSC Adv.* 10, 21839–21844. doi:10.1039/d0ra03424j

Zou, J., Wang, Y., Baryshnikov, G., Luo, J., Wang, X., Ågren, H., et al. (2022). Efficient dye-sensitized solar cells based on a new class of doubly concerted companion dyes. *ACS Appl. Mater. and Interfaces* 14, 33274–33284. doi:10.1021/acsami.2c07950